Theoretical study of a motor vehicle-pole impact

Robert Milner, Raphael Grzebieta and Roger Zou
Department of Civil Engineering, Monash University, Melbourne, Australia

Abstract

This paper presents a theoretical model investigating a car impact with a timber light pole. A theoretical model, even one greatly simplified, that identifies the significant parameters and can be used for routine pole design is a useful tool. The model proposed in this paper, compares its predictions with those of a commercial dynamic analysis package and presents the results of a parameter study that identifies the important pole parameters and quantifies their effect. The parameter study highlights the fact that the act of simply making a pole frangible will not, of its own, reduce vehicle decelerations to levels where car occupants are likely to survive. Pole mass also plays a significant role.

Keywords

Pole impact, frangible pole, Madymo pole model

Introduction

"Single vehicle crashes", where occupants are killed or seriously injured as a result of vehicles leaving the roadway, constitute a substantial proportion of the road crash problem. Around 35% of these crashes involve poles or trees [Corben et al (1997), Kloeden et al (1999), Haworth (1999), Federal office of Road Safety (1998)]. Hence there is a strong interest in motor vehicle – pole impacts. If a 20% reduction in the road toll is to be realised by 2010 then a strategy dealing with such crashes needs to be introduced.

It was speculated prior to commencing this study that pole strength and mass both played significant role in vehicle deceleration rates although their relative contributions and the manner in which they contributed were, initially, unclear. This paper is specifically concerned with the following.

- Identification of the parameters that affect motor vehicle deceleration rates during a pole impact and quantification of their effect.

- Development of a closed form solution, based on simplifying assumptions, that adequately describes the impact event and enables the designers of frangible poles to predict the peak deceleration rates without having to resort to expensive commercial computer packages. The simplified model has also proven useful in describing the sequence of events that are sometimes masked by numerical solutions.

- Comparison of the prediction of closed form solution with that provided by a commercial dynamic analysis package, MADYMO. MADYMO is a general purpose engineering computer program using multibody and finite element techniques. It is used, inter alia, to simulate vehicle collisions for use in vehicle and road-side furniture design.

Development of the closed form solution

A typical pole is illustrated in Fig 1. It has an above ground length, L, and is struck at height, h, above ground level, typically of the order of 0.5 - 0.6*m*. It is assumed that the based shear strength will be exceeded at some stage of the vehicle impact and that the pole therefore ruptures in shear. In the pre-rupture phase it is assumed that the pole acts as a rigid object. While this is not completely correct it is nearly the case. In reality the soil would deform slightly but this is thought not to have a significant impact on vehicle decelerations. Furthermore, the effect of soil deformation can be added easily to the analysis but choosing an appropriate value introduces a number of imponderables.

There are two complications associated with analysing vehicle-pole impacts. Firstly, the rupture of the pole changes the physical system. Pre-rupture pole dynamic effects are negligible and ignored but post-rupture pole dynamics become dominant. Secondly the nature of vehicle response to impact changes sharply during the impact event as shown in Fig 2. The early response involves the vehicle crumpling and cushioning the impact. Once the pole penetrates the vehicle more than approximately 400 *mm* the vehicle becomes much stiffer due to contact with the engine and stiffer parts of the vehicle, leading to rapidly increasing vehicle decelerations. Any

realistic modeling must consider this bi-linear vehicle response. These complications lead to bilateral categorisation of impact sequences. Sequence 1 (infrangible poles) is associated with: Stage 1-2 where initial impact occurs and continues until the vehicle has fully crumpled (engine strike); Stage 2-3 where the force resistance suddenly rises until rupture of pole occurs; and Stage 3-4 where the force continues to rise because the vehicle continues to interact with the severed pole trying to overcome the pole's inertia. Sequence 2 (frangible poles) is associated with: Stage 1-2 where initial impact and some crumple occurs up to the moment the pole ruptures; Stage 2-3 where vehicle crumpling is completed (engine strike) as it continues to interact with the severed pole and its inertia; Stage 3-4 where the force suddenly rises on completion of vehicle crush and it then continues to interact with the severed pole's inertia, i.e. trying to accelerate the pole.

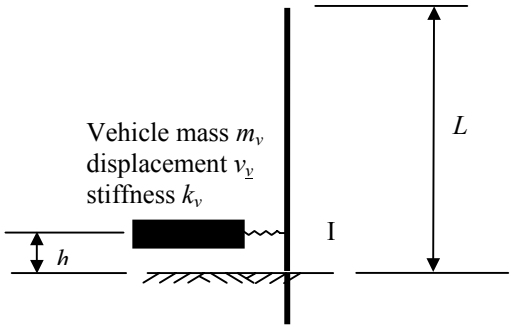

Figure 1 Idealised pole model under study.

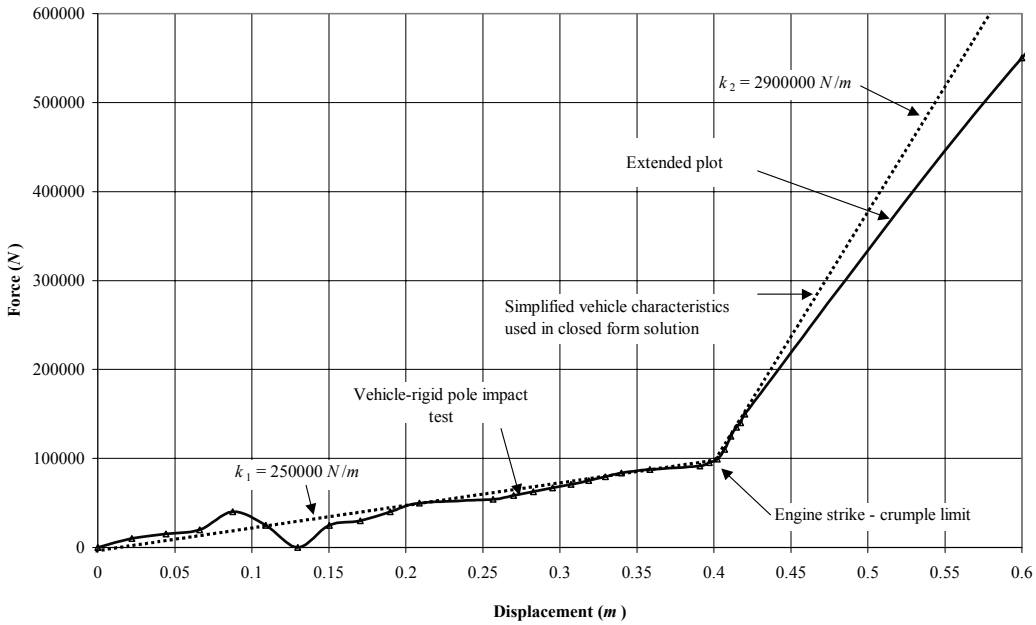

Figure 2 Typical idealised vehicle deformation response in a pole impact.

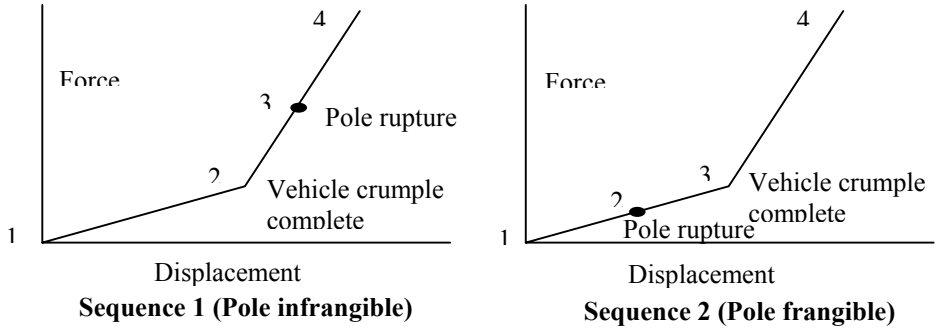

Sequence 1 (Pole infrangible) **Sequence 2 (Pole frangible)**

Figure 3 Impact sequences.

The governing differential equations and their solutions are provided in the Appendix. The nature of the impact means that it is an initial value problem, ie, all boundary conditions are defined at the commencement of each of the stages 1-2, 2-3, and 3-4. By computing the time to the commencement of each stage and the initial boundary conditions, the events in the next stage of impact can be computed using the appropriate equations given in the Appendix. The following notation is used in describing the impact event.

v_v, v_p, θ, $\dot{v}_v$, $\dot{v}_p$, $\dot{\theta}$, $\ddot{v}_v$, $\ddot{v}_p$, $\ddot{\theta}$ = vehicle linear displacement, pole linear displacement, pole angular displacement, (vehicle, pole, pole angular) velocity, (vehicle, pole and pole angular) acceleration.

t = time.

m_v, m_p, I_p = vehicle linear inertia (mass), pole linear inertia, pole angular inertia (moment of inertia)

$\dot{v}_0$ = impact velocity, i.e., the speed of the vehicle at the moment of impact.

v_{v1}, v_{v2}, v_{v3} = vehicle displacement measured from the initial pole contact point to the commencement of stages 1-2, 2-3, 3-4 respectively.

v_{p1}, v_{p2}, v_{p3}, θ_1, θ_2, θ_3 = pole linear displacement in the horizontal direction and angular displacement at the commencement of stages 1-2, 2-3, 3-4 respectively.

$\dot{v}_{v1}$, $\dot{v}_{v2}$, $\dot{v}_{v3}$ = vehicle velocity measured from the initial pole contact point to the commencement of stages 1-2, 2-3, 3-4 respectively.

$\dot{v}_{p1}$, $\dot{v}_{p2}$, $\dot{v}_{p3}$, $\dot{\theta}_1$, $\dot{\theta}_2$, $\dot{\theta}_3$ = pole linear velocity in the horizontal direction and angular velocity at the commencement of stages 1-2, 2-3, 3-4 respectively.

k_1, k_2 = vehicle stiffness characteristics before and after engine strike (crumple limit).

t_1, t_2, t_3 = time markers to start of stages 1-2, 2-3, 3-4.

t_C, t_R = time to engine strike, pole rupture.

ω, λ = fundamental frequency of the vehicle-pole system before and after pole rupture – these values change depending on the vehicle stiffness.

Sequence 1 impact (infrangible pole)

Stage 1-2 (Initial impact to completion of crumple)

Boundary conditions at the start of Stage 1-2 are $t_0 = t_1 = 0$, $v_{v0} = 0$, $\dot{v}_{v0} = \dot{v}_0$. Equation A4 where $\omega = \omega_1 = \sqrt{k_1/m_v}$ is then used to compute v_v. Equation A4a then simplifies to $v_v = (\dot{v}_0/\omega_1) sin\,\omega_1 t$. Velocities and accelerations are obtained by differentiation.

Stage 2-3 (After completion of crumple to moment of pole rupture)

Boundary conditions at the start of Stage 2-3 are $t_0 = t_2 = t_C = (1/\omega_1) sin^{-1}(\omega_1 v_C/\dot{v}_0)$ where v_C = crumple penetration = 0.4*m* (see Fig 2), $v_{v0} = (\dot{v}_0/\omega_1) sin\,\omega_1 t_2$, $\dot{v}_{v1} = \dot{v}_0\, cos\,\omega_1 t_2$. Equation A4a is used to compute v_v during this stage where $\omega = \omega_2 = \sqrt{k_2/m_v}$, $F_0 = (k_2 - k_1) v_C$. Velocities and accelerations are again obtained by differentiation.

Stage 3-4 (Post pole rupture)

The time to rupture cannot be computed simply by a closed form formula. If a spread sheet is used, it can be obtained simply by observing the time at which $V_R = |m_v \ddot{v}_v|$. If using other coding equation A4c must be solved to extract t_R with $V_R = |m_v \ddot{v}_v|$. This is a non-linear algebraic expression that has no closed form solution. A simple bisection approach can be used to extract t_R. Another way is to assume that $t_0 = t_3 = t_R$ is known. Boundary conditions at the start of Stage 3-4 are given by equations A4a and A4b with $t = t_3$, and

$\omega = \omega_2 = \sqrt{k_2/m_v}$. Equation A14 then provides displacements during Stage 3-4. Velocities and accelerations are obtained by differentiation.

Sequence 2 impact (frangible pole)

Stage 1-2 (Initial impact to pole rupture)

As for Sequence 1.

Stage 2-3 (Pole rupture to completion of crumple)

Boundary conditions at the start of Stage 2-3 are $t_0 = t_2 = t_R \quad = (1/\omega_1) sin^{-1}(V_R/\omega_1 m_v \dot{v}_0)$, $v_{v1} = (\dot{v}_0/\omega_1) sin\omega_1 t_1$, $\dot{v}_{v1} = \dot{v}_0 cos\omega_1 t_1$. Equation A14a is then used to compute v_v .

Stage 3-4 (Post completion of crumple and pole rupture)

Again the time to crumple cannot be computed simply by a closed form solution. If a spread sheet is used, it can be obtained simply by observing the time at which $V_R = |m_v \ddot{v}_v|$, otherwise a solution procedure analogous to Sequence 1 can be adopted.

Typical vehicle-pole impact event

The characteristics of a typical pole impact are depicted in Figs 4 to 6.

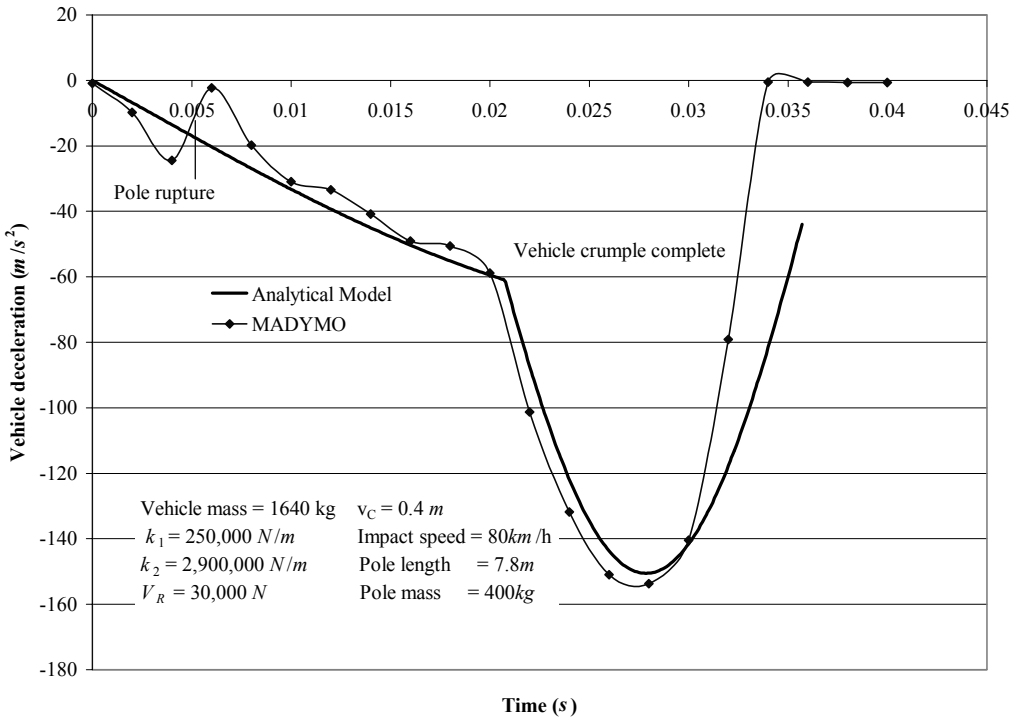

Figure 4 Vehicle deceleration.

The principal interest lies with the vehicle deceleration, shown in Fig 4 featuring results from both MADYMO and the analytical solution. In this example, a pole rupture strength of 30 *kN* has been adopted. At this level the pole is considered frangible yet has sufficient shear capacity to support the head loads commonly specified by power distribution companies. Other parameters used in the example include vehicle impact velocity 80 *km*/*h*, pole mass 400 *kg* (above ground), pole length 7.8 *m* above ground, vehicle mass 1640 *kg* and it is assumed that the pole is struck at a height of 0.5 *m* above ground level.

The pole ruptures approximately 5 *ms* after initial contact with the vehicle decelerating at approximately 2*g* after which the vehicle deceleration continues to rise due to pole inertia. At 20.5 *ms* the pole has penetrated the vehicle by a distance of 0.4 *m* (see Fig 2) at which point the crumple limit (Fig 2) has been reached. There now follows a sharp rise in vehicle deceleration to a peak around 15*g* in this case. The rapidly rising deceleration occurs on due to the sudden rise of vehicle stiffness, associated with engine strike. The whole sequence of events highlights the fact that the provision of pole frangibility on its own is insufficient to reduce deceleration rates to survivable levels, typically taken as less than 20*g*. Pole mass also plays an important role.

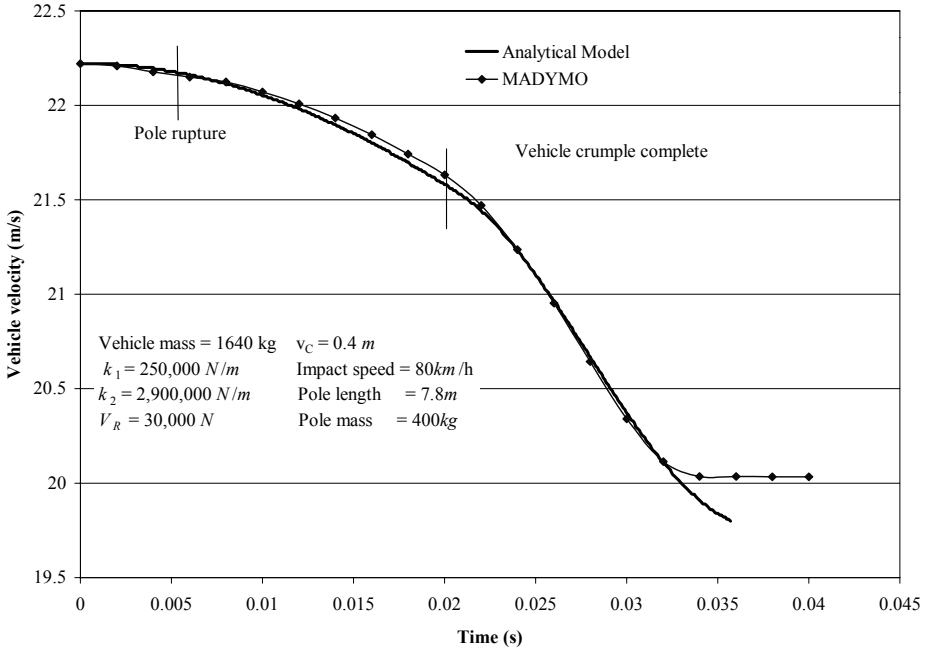

Figure 5 Vehicle velocity.

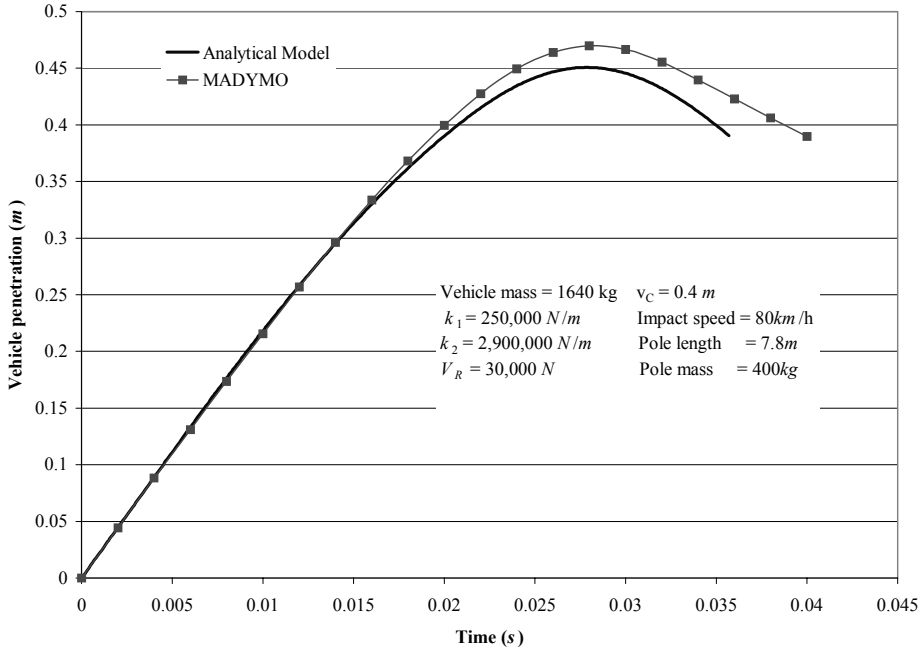

Figure 6 Vehicle penetration.

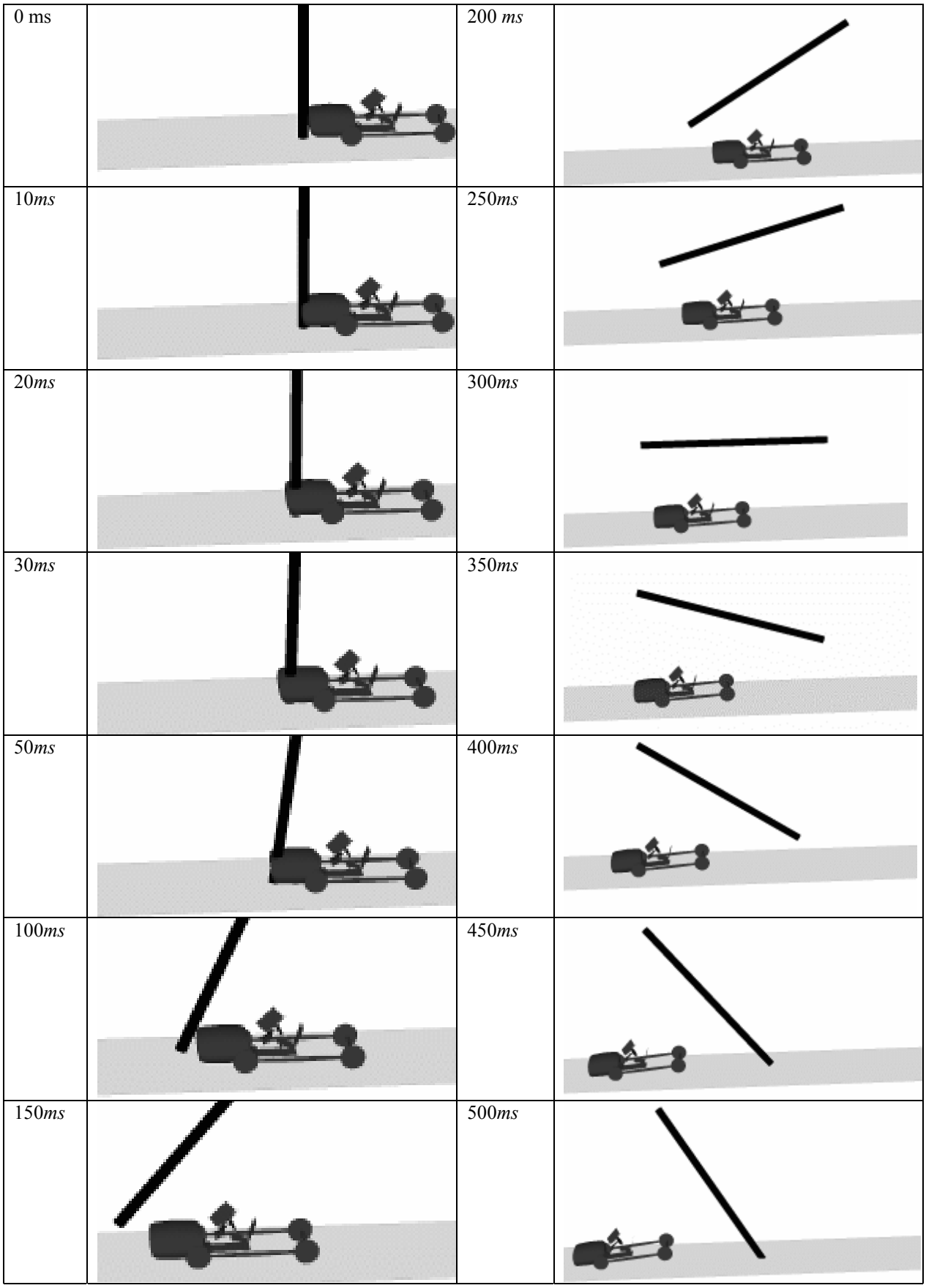

Figure 7 MADYMO Vehicle–pole impact. Input parameters correspond to those indicated in Figs 4-6.

Parametric studies of typical vehicle-pole impacts

MADYMO was used to study the effect of varying the principal input parameters. Typical poles have the characteristics shown in Table 1. Pole mass details are estimates but are sufficiently accurate for the purposes of this study. Fig. 7 shows a typical animation sequence where some of the images have been enlarged for clarity. The vehicle mass (1640 *kg*) and stiffness characteristics (Fig 2) were kept constant during the parametric studies reported in Table 2. Table 2 shows the resulting peak vehicle deceleration for various pole types. It is clear that even if a pole is frangible the decelerations will be excessive for poles with a mass of 800 kg or more.

Table 1 Indicative pole specifications. Mass figures are only approximate.
Concrete poles are hollow whereas timber poles are solid.

Pole length range - above ground (*m*)	Ultimate head load capacity (*kN*)	Ultimate bending moment capacity (*kNm*)	Ultimate torsion moment capacity (*kNm*)	Pole mass of above ground segment (*kg*)	
				Concrete	Timber
6 – 12	6	36 – 72	2.4	580-1150	400-900
7 – 14	10	70 – 140	5.0	900-1900	
7 – 17	16	112 – 270	8.0	1000-3100	
7 –20	24	168 – 480	8.0	1250-4400	

Table 2 Parametric study carried using MADYMO.

Input Parameters				**Results**	
Pole Base Peak Force (*N*)	Pole Mass (*kg*)	Vehicle Velocity (*km/h*)	Vehicle Mass (*kg*)	Peak Vehicle Deceleration (*g*)	Vehicle Velocity After Impact (*m/s*)
10000	400	80	1640	14.5	19.99
30000	400	80	1640	15.4	19.99
90000	400	80	1640	21.9	19.3
30000	200	80	1640	5.6	21.05
30000	400	80	1640	15.4	19.99
30000	800	80	1640	26.0	17.75
30000	**400**	**80 (22.22m/s)**	**1640**	**15.4**	**19.99**
30000	400	60 (16.67m/s)	1640	6.9	15.04
30000	400	50 (13.89m/s)	1640	5.1	12.52
30000	400	40 (11.11m/s)	1640	3.8	9.98
30000	400	30 (8.34m/s)	1640	3.1	7.29
30000	200	80	1640	5.6	21.09
30000	200	60	1640	4.2	15.78
30000	200	40	1640	3.0	10.46
30000	200	30	1640	2.2	7.74

Discussion and conclusions

The road deaths involving single vehicle impacts with poles has the potential to be reduced but the use of frangible poles with reduced base shear capacities will not on its own bring this about. It is essential pole mass also be limited.

The analytical / semi-closed form solution is adequate for determining the peak deceleration of the vehicle and could be used as a basis for routine design of frangible poles. Because the closed form solution equations is based on linear geometry it is not suitable for predicting the path followed by the pole once the displacements become large. There is evidence of a divergence of the two solutions (closed form and MADYMO) after peak vehicle deceleration has occurred due to the linearity of the geometry.

With frangible poles the impact process will tend to follow Sequence 1 with pole rupture occurring well before crumple limit is reached and engine strike occurs. A closed form solution for the time to engine strike is not

available. This is easily obtained by simple numerical techniques for the solution of non-linear algebraic equations, such as the bisection method.

MADYMO or a similar analysis package is required for assessing the collateral damage resulting from the pole's post-rupture motion. Collateral damage is less likely with power poles owing to the restraint of the conductors. Collateral damage could conceivably involve striking bystanders or nearby property or, depending on the impact velocity, falling on the impacting vehicle where the post-rupture velocity is insufficient to clear the falling pole.

References

Corben, B., Deery H., Mullan N. and Dyte D. (1997). *The General Effectiveness of Countermeasures for Crashes Into Fixed Roadside Objects*, Report No. 111, Monash University Accident Research Centre, Clayton, Australia.

Federal Office of Road Safety (FORS). "*Monthly Bulletin*", Statistical Publications, Canberra, Australia, August 1998.

Haworth, N. (1999) *Fatal Single Vehicle Crashes Study*, Proc. 6th ITE International Conference Road Safety & Traffic Enforcement: Beyond 2000, Institution of Transportation Engineers, Sept., Melbourne.

Kloeden C.N., McLean A.J., Baldock M.R.J. & Cockington A.J.T., (1999), *Sever and Fatal Car Crashes due to Roadside Hazards*, Report for Motor Accident Commission, May, South Australia.

Marzougui, D, Eskandarian, A, Meczkowski, L, "Analysis and evaluation of a redesigned 3"x3" slipbase sign support system using finite element simulations", IJCrash 1999 Vol 4 No 1, pp 7 – 16.

TNO Automotive, "MADYMO User's Manual 3D", Version 5.4, May 1999

Appendix – closed form solution

Pre-rupture solution

In the pre-rupture stage the pole is taken as infinitely rigid. The governing differential equation has the form

$$m_v \ddot{v}_v + k v_v - F_0 = 0 \qquad \text{A1}$$

where $F_0 = 0$ during vehicle crumple, $F_0 = (k_2 - k_1) v_C$ after crumple is complete, and v_C = vehicle crumple displacement. Equation A1 may be rewritten as

$$\ddot{v}_v + \omega^2 v_v = \frac{F_0}{m_v} \qquad \text{A2}$$

This has the solution

$$v_v = a \sin\omega t + b \cos\omega t + \frac{F_0}{\omega^2 m_v} \qquad \text{A3}$$

If the velocity, $\dot{v}_{v0}$ and displacement, v_{v0}, are specified at a time t_0 the final solution is

$$v_v = \left(\frac{\dot{v}_{v0}}{\omega} \cos\omega t_0 + \left(v_{v0} - \frac{F_0}{\omega^2 m_v} \right) \sin\omega t_0 \right) \sin\omega t + \left(-\frac{\dot{v}_{v0}}{\omega} \sin\omega t_0 + \left(v_{v0} - \frac{F_0}{\omega^2 m_v} \right) \cos\omega t_0 \right) \cos\omega t \qquad \text{A4a}$$

$$\dot{v}_v = \omega\left(\frac{\dot{v}_{v0}}{\omega}cos\,\omega t_0 + \left(v_{v0} - \frac{F_0}{\omega^2 m_v}\right)sin\,\omega t_0\right)cos\,\omega t - \omega\left(-\frac{\dot{v}_{v0}}{\omega}sin\,\omega t_0 + \left(v_{v0} - \frac{F_0}{\omega^2 m_v}\right)cos\,\omega t_0\right)sin\,\omega t$$

A4b

$$\ddot{v}_v = -\omega^2\left(\frac{\dot{v}_{v0}}{\omega}cos\,\omega t_0 + \left(v_{v0} - \frac{F_0}{\omega^2 m_v}\right)sin\,\omega t_0\right)sin\,\omega t - \omega^2\left(-\frac{\dot{v}_{v0}}{\omega}sin\,\omega t_0 + \left(v_{v0} - \frac{F_0}{\omega^2 m_v}\right)cos\,\omega t_0\right)cos\,\omega t$$

A4c

Post-rupture

After rupture, let u_t, v_t, u_b, v_b = displacement of the pole at tip and base (ground) level, θ = rotation of the pole, u_p, v_p = displacement of the centre of gravity of the pole as shown in Fig A1. Thus the pole geometry is described by the following parameters.

Displacements	**Velocities**	**Accelerations**
Pole Tip $u_A = u_p$	$\dot{u}_A = \dot{u}_p$	$\ddot{u}_A = \ddot{u}_p$
$v_A = v_p - 0.5L\theta$	$\dot{v}_A = \dot{v}_p - 0.5L\dot{\theta}$	$\ddot{v}_A = \ddot{v}_p - 0.5L\ddot{\theta}$
Pole Centroid $u_D = u_p$	$\dot{u}_D = \dot{u}_p$	$\ddot{u}_D = \ddot{u}_p$
$v_D = v_p + 0.5L\theta$	$\dot{v}_D = \dot{v}_p + 0.5L\dot{\theta}$	$\ddot{v}_D = \ddot{v}_p + 0.5L\ddot{\theta}$
Pole at Impact Point $u_I = u_p$	$\dot{u}_I = \dot{u}_p$	$\ddot{u}_I = \ddot{u}_p$
$v_I = v_p + (0.5L - h)\theta$	$\dot{v}_I = \dot{v}_p + (0.5L - h)\dot{\theta}$	$\ddot{v}_I = \ddot{v}_p + (0.5L - h)\ddot{\theta}$

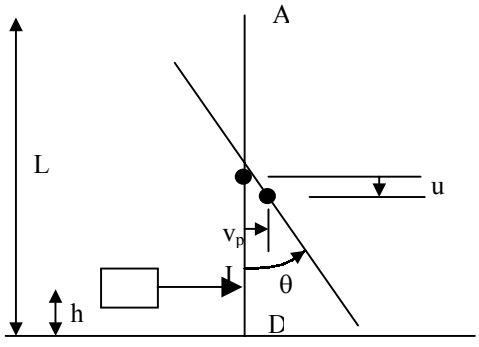

Figure A1 Parameters used to describe post-rupture pole geometry.

In the post-rupture stage both the pole and vehicle have inertia terms associated with them. There are three (ignoring vertical drop) simultaneous differential equations associated with them that in small displacements take the form

$$m_v\ddot{v}_v + kv_v - kv_p - k(0.5L - h)\theta - F_0 = 0 \qquad \text{A5}$$

$$m_p\ddot{v}_p - kv_v + kv_p + k(0.5L-h)\theta + F_0 = 0 \quad \text{A6}$$

$$\frac{m_pL^2}{12(0.5L-h)}\ddot{\theta} - kv_v + kv_p + k(0.5L-h)\theta + (0.5L-h)F_0 = 0 \quad \text{A7}$$

Adding equations A5 and A6 leads to $m_v\ddot{v}_v + m_p\ddot{v}_p = 0$ which is integrated twice to give

$$m_vv_v = -m_pv_p + At + B \quad \text{A8}$$

At time $t = t_0$, $\dot{v}_v = \dot{v}_{v0}$, $v_v = v_{v0}$, $\dot{v}_p = \dot{v}_{p0}$, $v_p = v_{p0}$. Hence

$$A = m_v\dot{v}_{v0} + m_p\dot{v}_{p0} \quad \text{A9}$$

$$B = m_vv_{v0} + m_pv_{p0} - At_0 \quad \text{A10}$$

Adding equations A6 and A8 leads to $\frac{I_p}{(0.5L-h)}\ddot{\theta} + m_v\ddot{v}_v = 0$ which is integrated twice to give

$$\frac{I_p}{(0.5L-h)}\theta + m_vv_v = Ct + D \quad \text{A11}$$

At time $t = t_0$, $\dot{v}_v = \dot{v}_{v0}$, $\dot{\theta} = \dot{\theta}_0$, $v_v = v_{v0}$, $\theta = \theta_0$. By analogy

$$C = m_v\dot{v}_{v0} + \frac{I_p}{(0.5L-h)}\dot{\theta}_0 \quad \text{A12}$$

$$D = m_vv_{v0} + \frac{I_p}{(0.5L-h)}\theta_0 - Ct_0 \quad \text{A13}$$

Equations A8 and A11 are substituted back into equation A5 to produce

$$\ddot{v}_v + k\left(\frac{1}{m_v+m_p}\frac{1}{}+\frac{(0.5L-h)^2}{I_p}\right)v_v = k\left(\frac{A}{m_vm_p}+\frac{(0.5L-h)^2}{I_pm_v}\right)t + k\left(\frac{B}{m_vm_p}+\frac{D(0.5L-h)^2}{I_pm_v}\right)+\frac{F_0}{m_v} \quad \text{A14}$$

which is rewritten as

$$\ddot{v}_v + \lambda^2v_v = Et + F \quad \text{A15}$$

where

$$\lambda^2 = k\left(\frac{1}{m_v+m_p}\frac{1}{}+\frac{(0.5L-h)^2}{I_p}\right) \quad \text{A16}$$

Equation A14 has the solution

$$v_v = a\sin\lambda t + b\cos\lambda t + \frac{E}{\lambda^2}t + \frac{F}{\lambda^2} \tag{A17}$$

$$\dot{v}_v = a\lambda\cos\lambda t - b\lambda\sin\lambda t + \frac{E}{\lambda^2} \tag{A18}$$

$$\ddot{v}_v = -a\lambda^2\cos\lambda t - b\lambda^2\cos\lambda t \tag{A19}$$

At time $t = t_0$, $\dot{v}_v = \dot{v}_{v0}$, $v_v = v_{v0}$.

$$a\sin\lambda t_0 + b\cos\lambda t_0 = v_{v0} - \frac{E}{\lambda^2}t_0 - \frac{F}{\lambda^2} = R_1 \tag{A20}$$

$$a\cos\lambda t_0 - b\sin\lambda t_0 = \frac{\dot{v}_{v0}}{\lambda} - \frac{E}{\lambda^3} = R_2 \tag{A21}$$

or

$$\begin{bmatrix} \sin\lambda t_0 & \cos\lambda t_0 \\ \cos\lambda t_0 & -\sin\lambda t_0 \end{bmatrix} \begin{Bmatrix} a \\ b \end{Bmatrix} = \begin{Bmatrix} R_1 \\ R_2 \end{Bmatrix} \tag{A22}$$

Equation A21 has the solution

$$\begin{Bmatrix} a \\ b \end{Bmatrix} = \begin{bmatrix} \sin\lambda t_0 & \cos\lambda t_0 \\ \cos\lambda t_0 & -\sin\lambda t_0 \end{bmatrix} \begin{Bmatrix} R_1 \\ R_2 \end{Bmatrix} \tag{A23}$$